

Role of chiral symmetry in a kicked Jaynes-Cummings model

Pinquan Qin^{1,*} and Hee Chul Park^{2,†}

¹*Department of Physics, Wuhan University of Technology, Wuhan 430070, China*

²*Center for Theoretical Physics of Complex Systems, Institute for Basic Science (IBS), Daejeon 34126, Republic of Korea*



(Received 30 May 2022; accepted 3 January 2023; published 19 January 2023)

We have studied the role of chiral symmetry in a periodically kicked Jaynes–Cummings (KJC) model by freezing an initial phase. We show that commensurate kicks ($2\pi k$ periodicity with integer k) conserve the chiral symmetry in the KJC model under the resonant condition, while incommensurate kicks break the symmetry. The chiral symmetry preserves the phase of an initial state against phase fluctuations during the dynamical evolution, but broken chiral symmetry erases the initial phase. The frozen phase is preserved within a finite evolution time for slight deviations of the kick period from an integer multiple of 2π and small variations of detuning from the resonant condition. The chiral symmetry-protected phase information is noteworthy as it provides various uses in quantum computation and information.

DOI: [10.1103/PhysRevA.107.013712](https://doi.org/10.1103/PhysRevA.107.013712)

I. INTRODUCTION

For decades, the strong couplings between light and matter have been studied for implementing quantum information across various intensities, such as strong coupling, ultrastrong coupling, and deep-strong coupling in Jaynes–Cummings (JC) models [1–4]. Although the JC model has been used to examine the classical aspects of spontaneous emission and reveal Rabi oscillation, the model has also been extended to a quantum mechanical model of a two-level atom in a single-mode bosonic field. The evolutionary version of the quantum JC model—the driven JC model—has attracted a lot of research attention and gives rise to interesting phenomena such as electromagnetic squeezing [5], vacuum Rabi splitting [6,7], photon blockade [8–10], symmetry breaking [11], rich structures of multiphoton resonances [12,13], and the readout of qubits [14,15]. The driven JC model belongs to the periodically driven system called the Floquet system [16–18]. The periodically driven system has garnered many research efforts in quantum physics—for example, to treat dynamical systems [19,20], extend the synthetic dimension [21,22], and explore topological phases [23–26] and thermodynamics [27–29]. Typically, the commensurability of the modulation function of the Floquet system offers not only dynamical phenomena like quantum resonance and dynamical localization [30,31] but also opto-electro-mechanics in hybrid devices [32,33].

In addition, chiral symmetry [34], described as invariance under parity transformation by a Dirac fermion, plays key roles in quantum mechanics, such as conservation and topological classification [35,36]. Chiral symmetry can create a class of topological phases in one-dimensional (1D) systems without both time-reversal and particle-hole symmetries [37].

The unitary operator Γ characterizes whether the system satisfies chiral symmetry through the relation $\Gamma U \Gamma^\dagger = U^{-1}$, where Γ is unitary/Hermitian and obeys $\Gamma^2 = 1$, and $U = e^{-iHt/\hbar}$ is the Floquet operator describing the time evolution of the Hamiltonian H [35]. Most recent research has focused on Floquet topological phases in driven models, such as the kicked Harper model [38–41], double kicked rotor [42–44], and quantum walk [35,45–48], with chiral symmetry. The interplay between time modulation and chiral symmetry in a quantum system not only provides topological phases but also offers more possibilities to develop quantum technology and be applied to quantum devices.

In this work, we designed a quantum JC model combined with time-periodic discrete potentials, called a kicked Jaynes–Cummings (KJC) model. The KJC model under the resonant condition shows that commensurate kicks, namely, $2\pi k$ periodicity with an integer k , conserve the chiral symmetry, while incommensurate kicks break the symmetry. The chiral symmetry enforces symmetric pairs of eigenphases and eigenstates of the Floquet operator, $(-\varepsilon_\alpha, \varepsilon_\alpha)$, indicated by the states α . Moreover, the amplitude distribution coefficients of paired eigenstates are complex conjugates with additional global phases. But most interestingly, by a direct derivation, the initial phase encoded in the initial state is protected from phase fluctuations; more specifically, the chiral symmetry freezes the initial phase in the KJC model concerning the time evolution. On the other hand, breaking the chiral symmetry washes out the initial phase. Notably, this frozen-phase effect is preserved against small perturbations within a finite time evolution.

This paper is organized as follows. In Sec. II, we introduce the JC model with a periodically driven potential. In Sec. III, we characterize the chiral symmetry of the KJC model. Then, Sec. IV presents the eigenstates of the Floquet operator with chiral symmetry, and Sec. V gives the results of the chiral symmetry-protected frozen phase. Section VI summarizes our results. Two appendices then follow for the derivations of the

*qinpqcu@whut.edu.cn

†hcpark@ibs.re.kr

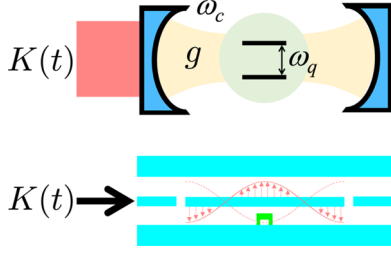


FIG. 1. Schematic diagrams of driven Jaynes–Cummings models. The upper panel shows a coupled system with a two-level atom and an optical cavity, and the lower panel depicts a coupled system with a circuit QED and transmission line. The external driving potential $K(t)$ can be sinusoidal oscillation or discrete kicks.

amplitude distribution coefficients of the eigenstates and state evolution.

II. JC MODEL WITH PERIODICALLY DRIVEN POTENTIAL

The driven JC model can be manipulated in several ways, e.g., as a two-level atom within an optical cavity, a circuit quantum electrodynamics (QED) with superconducting transmission line resonators, and a superconducting quantum interference device (SQUID) with resonators, two of which are shown in Fig. 1. The JC Hamiltonian describes interactions between a cavity and a two-level system, $H_{JC} = H_c + H_a + H_g$. The cavity Hamiltonian is defined by the free electromagnetic field, $H_c = \hbar\omega_c a^\dagger a$, where ω_c is the electromagnetic field frequency of the cavity and a/a^\dagger is the annihilation/creation operator of the field satisfied by $[a, a^\dagger] = 1$. The two-level system is described by an atomic Hamiltonian, $H_a = \hbar\omega_q \sigma_z/2$, where ω_q is the atomic transition frequency and σ_z is the Pauli matrix describing the two states. The two subsystems $H_0 = H_c + H_a$ are coupled by the interaction Hamiltonian, implying the conservation of the number of excitations in the system concerning the rotational wave approximation. The coupling Hamiltonian is $H_g = g(a\sigma_+ + a^\dagger\sigma_-)$, where g is the atom–cavity coupling strength and $\sigma_\pm = (\sigma_x \pm i\sigma_y)/2$ is the raising/lowering atomic operator (below $\hbar = 1$). The driven JC Hamiltonian reads

$$H = H_{JC} + K(t/T, \xi), \quad (1)$$

where ξ and T are the strength and the period of the driven potential, respectively. The time-dependent term is proportional to the displacement operator $(a + a^\dagger)$ and the time-periodic function. Let us consider periodic kicks by using a delta function series as a discrete driving potential,

$$K(t/T, \xi) = \xi(a + a^\dagger) \sum_n \delta(t/T - n). \quad (2)$$

Here, we have two possible degrees of freedom: whether T is commensurate to an integer multiple of 2π or not.

Experimentally, this system can be realized by replacing the amplitude of the external drive with a sinusoidal function, $K(t) = \xi \cos(\omega t)(a + a^\dagger)$, where $\omega = 2\pi/T$, which we call a sinusoidal Jaynes–Cummings (SJC) model. The SJC Hamiltonian is demonstrated by coupling a superconducting charge qubit to a transmission line resonator [49]. The qubit can be

measured and coherently controlled by applying microwaves $K(t)$ to the input port of the resonator. Technologically, this external time-dependent driving amplitude can be replaced by a train of pulses with short durations and a suppression of T [50].

III. CHIRAL FLOQUET OPERATOR IN THE KJC MODEL

A periodic time-dependent Hamiltonian can be solved by the Floquet theorem concerning the periodic wave function and the quasi-energy. The wave function of the Schrödinger equation is $\Psi_\alpha(t) = e^{-i\mathcal{E}_\alpha t} \Phi_\alpha(t)$, where the Floquet wave function is periodic, $\Phi_\alpha(t) = \Phi_\alpha(t + T)$, and \mathcal{E}_α is the quasi-energy [51–54]. When we define the time evolution operator $U(t', t)$ with the Hamiltonian for the wave function, $U(t', t) = \mathcal{C} \exp(-i \int_t^{t'} H(\tau) d\tau)$, the Floquet wave function evolves by $U(t + T, t) \Phi_\alpha(t) = e^{-i\mathcal{E}_\alpha T} \Phi_\alpha(t)$, where we could get the spectrum of the quasi-energy from the eigenphase of the Floquet operator, $\varepsilon_\alpha = \mathcal{E}_\alpha T$.

The Floquet operator of the KJC model in the time interval $[0_-, T_-]$ has the following form under the commutation relation:

$$U(T_-, 0_-) = e^{-iH_c T} e^{-iK_V T}, \quad (3)$$

where $K_V = \xi(a + a^\dagger)$ and the subscript of T and 0 and $-$ means a little less time. Further, the free Hamiltonian H_0 and the coupling Hamiltonian H_g commute each other under the resonance condition $\omega_q = \omega_c = 1$. We can rewrite the Floquet operator separately as

$$U(T_-, 0_-) = e^{-iH_0 T} e^{-iH_g T} e^{-iK_V T}. \quad (4)$$

When the period of the kicked potential is commensurate to $2k\pi$, the chiral symmetry operator can be defined as

$$\Gamma = e^{i\pi a^\dagger a} e^{-i2k\pi\xi(a+a^\dagger)}, \quad (5)$$

where k is an integer. In order to prove that the Floquet operator satisfies the symmetry, let us separate the Floquet operator into two parts: $U(T_-, 0_-) = U_0 U_1$, where $U_0 = e^{-iH_0 T}$, and $U_1 = e^{-iH_g T} e^{-iK_V T}$. The first part of the Floquet operator U_0 gives the global constant for the eigenstate of H_0 as the basis $|n, \eta\rangle$, so that it does not make any physical difference as $U(T_-, 0_-) = \sum_{n, \eta=\pm} |n, \eta\rangle \langle n, \eta| U(T_-, 0_-) = (-1)^k U_1$, where n is the photon occupation number of the cavity and $\eta = \pm 1$ indicates the ground or excited state of the atom. The second part of the Floquet operator U_1 satisfies $\Gamma U_1 \Gamma^\dagger = U_1^{-1}$ with the chiral symmetry operator through the relation $e^{i\pi a^\dagger a} e^{-i2k\pi g(a\sigma_+ + a^\dagger\sigma_-)} e^{-i2k\pi\xi(a+a^\dagger)} = e^{i2k\pi g(a\sigma_+ + a^\dagger\sigma_-)} e^{i2k\pi\xi(a+a^\dagger)} e^{i\pi a^\dagger a}$ based on the anticommutation relation $\{(a + a^\dagger), e^{i\pi a^\dagger a}\} = 0$. Finally, the Floquet operator is satisfied by the relation

$$\Gamma U(T_-, 0_-) \Gamma^\dagger = U^{-1}(T_-, 0_-), \quad (6)$$

which represents a conservation of the chiral symmetry.

Chiral symmetry guarantees that the eigenfunctions of the Floquet operator $U(T_-, 0_-)$ are $|\phi_\alpha\rangle$ and $\Gamma|\phi_\alpha\rangle$ for a pair of eigenphases, $(-\varepsilon_\alpha, \varepsilon_\alpha)$, respectively, as follows:

$$U(T_-, 0_-)|\phi_\alpha\rangle = e^{-i\varepsilon_\alpha} |\phi_\alpha\rangle, \quad (7)$$

$$U(T_-, 0_-)\Gamma|\phi_\alpha\rangle = e^{i\varepsilon_\alpha} \Gamma|\phi_\alpha\rangle. \quad (8)$$

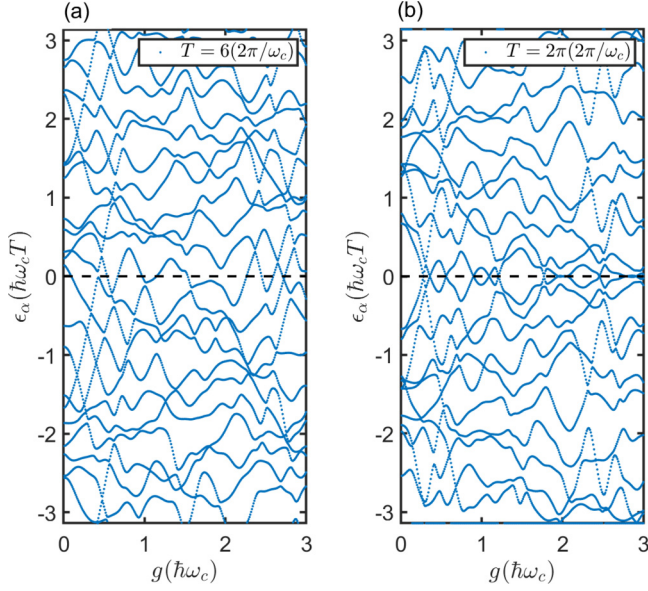


FIG. 2. Eigenphases ε_α of the Floquet operator $U(T_-, 0_-)$ vs the atom-cavity coupling strength g with the strength of the driven potential $\xi = 1.5$ and the period of the kicks, (a) $T = 6$ and (b) $T = 2\pi$.

Since the Floquet operator is the multiplication of exponential functions of operators, it is straightforward to define the corresponding matrix elements by inserting the eigenstate of H_g and K_V into Eq. (4). We can then directly obtain the eigenphases after diagonalizing the Floquet operator. Commensurately driven kicks provide symmetric eigenphases, while incommensurately driven kicks offer irregular eigenphases without symmetry. As shown in Fig. 2(a), when the kick period is $T = 6$, the eigenphases are not symmetric with a messy distribution. On the other hand, when the kick period is $T = 2\pi$, which is the commensurate time period, the eigenphases are perfectly symmetric according to the black dashed line at $\varepsilon_\alpha = 0$, as shown in Fig. 2(b).

IV. EIGENSTATES OF THE CHIRAL FLOQUET OPERATOR

As previously mentioned, the KJC model conserves chiral symmetry under the resonant condition and commensurate kicks. As follows from Eqs. (7) and (8), the eigenstates $|\phi_\alpha\rangle$ and $\Gamma|\phi_\alpha\rangle$ are connected by the eigenphases $(-\varepsilon_\alpha, \varepsilon_\alpha)$, respectively, due to the symmetry. This section will show a unique property of these paired eigenstates, the coefficients of which are based on the product states between the photon number and two-level state, and complex conjugates with additional global phases.

Let us construct the inner product between the Floquet eigenstates and the product states for each chiral symmetry partner as follows:

$$C_n^\eta(\alpha) = \langle n, \eta | \phi_\alpha \rangle, \quad (9)$$

$$\begin{aligned} D_n^\eta(\alpha) &= (-1)^n \langle n, \eta | \Gamma | \phi_\alpha \rangle \\ &= \langle n, \eta | e^{-i2k\pi\xi(a+a^\dagger)} | \phi_\alpha \rangle, \end{aligned} \quad (10)$$

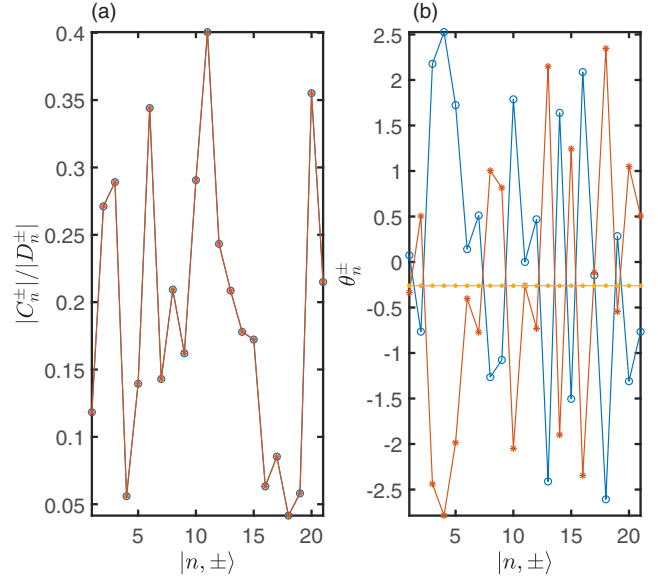


FIG. 3. (a) Absolute value and (b) phase of amplitude distribution coefficients C_n^η and D_n^η with respect to the basis $|n, \eta\rangle$ with eigenstate index $\alpha = 6$, atom-cavity coupling strength $g = 1.7$, driven potential strength $\xi = 1.5$, and period $T = 2\pi$. In both panels, the blue circle line and red star line indicate the absolute value and phase of C_n^η and D_n^η , respectively. In (b), the yellow dotted line indicates the summation of the phases of C_n^η and D_n^η , which gives the stable global phase $\theta_g = -0.2605$.

which are the amplitude distribution coefficients of Floquet eigenstates on the unperturbed basis. For a compact description, we will omit the symbol α in $C_n^\eta(\alpha)$ and $D_n^\eta(\alpha)$. The relation between the amplitude distribution coefficients of two chiral states is shown by

$$D_n^+ = (-1)^k e^{-i\varepsilon_\alpha} [C_n^+ \cos \beta_n + iC_{n+1}^- \sin \beta_n], \quad (11)$$

$$D_{n+1}^- = (-1)^k e^{-i\varepsilon_\alpha} [C_{n+1}^- \cos \beta_n + iC_n^+ \sin \beta_n], \quad (12)$$

where $\beta_n = 2k\pi g\sqrt{n+1}$ (see Appendix A). Here, we use the relation between the chiral operator Γ and coupling Hamiltonian H_g as follows:

$$\begin{aligned} \langle \phi_\alpha | (a^\dagger \sigma_- + a \sigma_+) \Gamma | \phi_\alpha \rangle &= \langle \phi_\alpha | (a^\dagger \sigma_- + a \sigma_+) e^{i\pi a^\dagger a} e^{-i2k\pi\xi(a+a^\dagger)} | \phi_\alpha \rangle \\ &= \langle \phi_\alpha | e^{i2k\pi\xi(a+a^\dagger)} (a^\dagger \sigma_- + a \sigma_+) e^{i\pi a^\dagger a} | \phi_\alpha \rangle. \end{aligned} \quad (13)$$

The above relation gives us $\sum_n (-1)^n \sqrt{n+1} P_n = 0$, where $P_n = D_n^+ (C_{n+1}^-)^* - D_{n+1}^- (C_n^+)^* + C_{n+1}^- (D_n^+)^* - C_n^+ (D_{n+1}^-)^*$. By combining Eqs. (11) and (12), the relation between the amplitude distribution coefficients is given by

$$\frac{D_n^+}{D_{n+1}^-} = \frac{(C_n^+)^*}{(C_{n+1}^-)^*}. \quad (14)$$

The amplitude distribution coefficient D_n^η is the complex conjugate of C_n^η with a global phase θ_g , since D_n^η and C_n^η are normalized—namely, $D_n^\eta = e^{i\theta_g} (C_n^\eta)^* = |C_n^\eta| e^{i(\theta_g - \theta_n^\eta)}$, where θ_n^η is the phase of C_n^η .

We can see numerically through Fig. 3 that the amplitude distribution coefficients of two states, $|\phi_\alpha\rangle$ and $|\psi_\alpha\rangle =$

$e^{-i2k\pi\xi(a+a^\dagger)}|\phi_\alpha\rangle$, are a complex conjugate pair with a global phase, which is independent on the basis $|n, \eta\rangle$. The yellow dotted line in Fig. 3(b) indicates the summation of the phases of all eigenstates, leading to the global phase.

V. CHIRAL SYMMETRY PROTECTED FROZEN PHASE

The time evolution of the chiral KJC model exhibits a peculiar phenomenon through the eigenphases and eigenstates of the Floquet operator. The chirality in this model tightens the phase fluctuation of the initial phase, which encodes a single state as an initial state by analyzing the time evolution of the states. This means that a frozen-phase effect is observed in the dynamical evolution of the KJC model under chiral symmetry.

The time evolution during $t = [0_-, MT_-]$ is defined by $|\Psi(M)\rangle = (U)^M|\Psi(0)\rangle$, and the final state can be expanded by the eigenstates of the Floquet operator $|\phi_\alpha\rangle$, where $|\Psi(0)\rangle$ is the initial state and M is an integer. The final state after M kicks forms as follows:

$$|\Psi(M)\rangle = \sum_{\alpha} e^{-i\varepsilon_{\alpha}MT} \langle\phi_{\alpha}|\Psi(0)\rangle |\phi_{\alpha}\rangle. \quad (15)$$

Here, we take the initial state $|\Psi(0)\rangle = e^{i\theta_0}|n_0, +\rangle$, which is the n_0 photon number state and excited atomic state with an initial phase θ_0 . Considering the properties of chiral eigenphases and eigenstates, we change the basis,

$$|\Psi(M)\rangle = \sum_{n, \eta=\pm} \mathcal{P}_n^\eta(M) |n, \eta\rangle, \quad (16)$$

where $\mathcal{P}_n^\eta(M)$ is the distribution function. The amplitudes of the distribution functions of the final state at the evolution time MT are shown in Fig. 4. In the case of the $T = 6$ kick period, the time evolution of the wave function is randomly fluctuating due to the incommensurate kick period. Surprisingly, in the case of the $T = 2\pi$ kick period as well, the time evolution of the wave function also presents fluctuating behavior. The amplitudes fluctuate randomly for the KJC model whether the period of kicks is incommensurate or commensurate. Seemingly, the reason for this is that the eigenstates of the Floquet operator are also randomly distributed due to the quasi-periodicity of the overlap functions, as shown in Fig. 3(a), even though the kick period is commensurate. In stark contrast, the phases of the final state are distinguished from the amplitudes of the distribution functions. For the kick period 2π , the phases of the distribution function of the state are unchanged over the dynamical evolution, as shown in Figs. 4(c) and 4(d), while for the kick period $T = 6$, the phases fluctuate. It turns out that the phases of the even-numbered states, $\text{mod}(n_0 + n, 2) = 0$, are fixed by the blueish color $\theta = \theta_0 = 0.5$ according to the dynamical evolution, and the phases of the odd-numbered states, $\text{mod}(n_0 + n, 2) = 1$, are designated by the yellowish color, $\theta = \theta_0 + \pi/2 = 2.071$ in Fig. 4(d), where $\text{mod}(\cdot, 2)$ is the modulo function for 2.

We can show a clear analytical derivation of the state evolution by separating the Floquet eigenstates into two groups of chiral states (see Appendix B). For the even $n_0 + n$, the

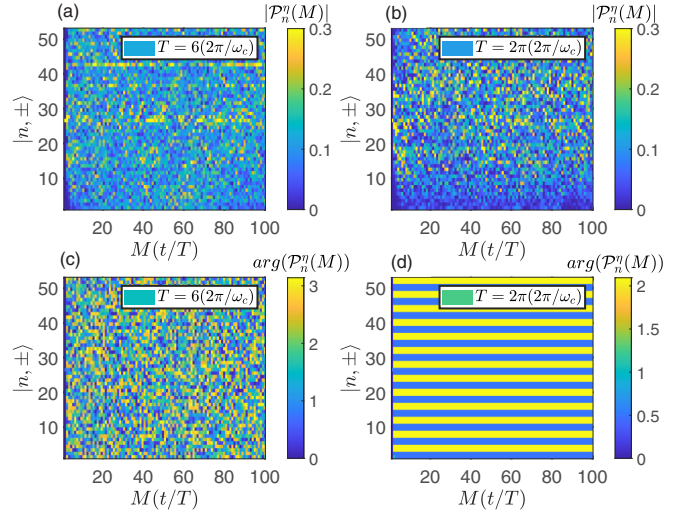


FIG. 4. (a) and (b) Amplitudes and (c) and (d) phases of the distribution function $\mathcal{P}_n^\eta(M)$ of the final state with respect to evolution time MT and the basis $|n, \eta\rangle$ with initial phase $\theta_0 = 0.5$ and initial state $n_0 = 12$. Other parameters are atom-cavity coupling strength $g = 1.7$ and driven potential strength $\xi = 1.5$. The periods of the kicks are $T = 6$ and $T = 2\pi$ in (a), (c) and in (b), (d), respectively. In (d), the blue color indicates the phase of the even state $\theta = \theta_0$, while the yellow color indicates the phase of the odd state $\theta = \theta_0 + \pi/2 = 2.071$.

coefficients of the basis are calculated by

$$\mathcal{P}_n^\eta(M) = e^{i\theta_0} \sum_{\alpha \in \mathbb{E}} [2|C_{n_0}^+ C_n^\eta| \cos Q_{n\alpha}^\eta(M)], \quad (17)$$

and for the odd $n_0 + n$,

$$\mathcal{P}_n^\eta(M) = i e^{i\theta_0} \sum_{\alpha \in \mathbb{E}} [-2|C_{n_0}^+ C_n^\eta| \sin Q_{n\alpha}^\eta(M)], \quad (18)$$

where $Q_{n\alpha}^\eta(M) = \varepsilon_{\alpha}MT + \theta_{n_0}^+ - \theta_n^\eta$ and \mathbb{E} is a set of absolute Floquet eigenvalues for grouping the states into bipartite parts, $\mathbb{E} = \{\alpha | \varepsilon_{\alpha} \geq 0\}$. Regardless of whether $n_0 + n$ is an even or odd number, the summations in Eqs. (17) and (18) are real numbers and the phase factors are θ_0 and $\theta_0 + \pi/2$ as constants. Thus, the evolved wave function keeps its initial phase. The chiral KJC model preserves the phase of the initial state during the dynamical evolution, i.e., freezes the initial phase.

Although we have attained that the frozen-phase effect exists in the chiral KJC model, we should know the stability of the frozen phase against deviations of the kick period from the commensurate frequency and detuning. In order to estimate the stability of the frozen phase, we define a quantity called the standard deviation of the phase as a function of the parameter ζ as follows:

$$\sigma(\zeta) = \sqrt{\frac{1}{M} \sum_m^M [\theta_m(\zeta) - \theta_0]^2}, \quad (19)$$

where $\theta_m(\zeta)$ is the phase of $\mathcal{P}_{n_0}^+(m)$ after m periods. In Fig. 5, $\zeta = \delta$ (a) and $\zeta = \Delta$ (b) give the perturbation of the kick period, $T = 2k\pi - \delta$, and the deviation of the atomic transition frequency as a detuning parameter, $\omega_q + \Delta$, respectively. The longer the time evolution, the greater the deviation of

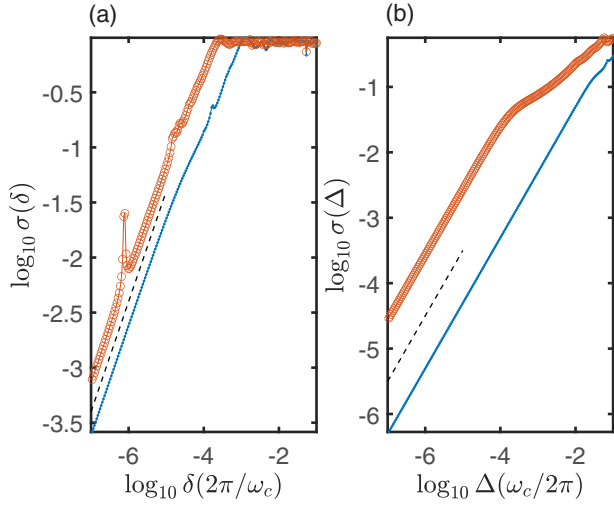


FIG. 5. Log-log plots of phase deviation $\sigma(\zeta)$ for the initial state as a function of perturbation ζ . (a) Plot with a deviation of kick period, $\zeta = \delta$, with $\Delta = 0$. (b) Plot with a variation of detuning parameter, $\zeta = \Delta$, with $\delta = 0$. Other parameters are initial phase $\theta_0 = 0.5$, atom-cavity coupling strength $g = 1.7$, and driven potential strength $\xi = 1.5$. The blue dotted line takes the evolution period $M = 100$, and the red circle line takes the evolution period $M = 500$. The dark dashed line is given as (a) $\log_{10} \sigma(\delta) = \log_{10} \delta + 3.6$ and (b) $\log_{10} \sigma(\Delta) = \log_{10} \Delta + 1.5$.

the evolutionary phase, as depicted by the blue dotted line ($M = 100$) and the red circle line ($M = 500$). Figure 5 shows that the standard deviation of the evolutionary phase increases linearly with the deviation of the time period and the detuning, and that the phase fluctuation becomes bigger as time goes on. As a result, the deviation of the frozen phase is linearly deviated according to the perturbation strength within a finite time scale.

VI. SUMMARY

In summary, we have studied the dynamical properties of a JC model with a periodically kicked potential under the resonant condition. The KJC model has chiral symmetry when the kick period is commensurate with 2π . We find that the corresponding chiral operator is defined by $\Gamma = e^{i\pi a^\dagger a} e^{-i2k\pi\xi(a+a^\dagger)}$ for the Floquet operator by the KJC Hamiltonian. Under chiral symmetry, the eigenphases of the Floquet operator are always a symmetric pair, $(-\varepsilon_\alpha, \varepsilon_\alpha)$. Furthermore, the amplitude distribution coefficients of the eigenstates corresponding to a pair of the eigenphases are complex conjugates with an extra global phase. These properties protect the initial phase of the initial state from phase fluctuations, giving the frozen-phase effect in the chiral KJC model. It is demonstrated that the frozen phase is preserved within a finite evolution time, even though the kick period and the detuning are slightly deviated from the commensurate period and the resonant condition, respectively. We expect that this frozen-phase effect exists in other systems with chiral symmetry, which can be proper candidates for phase information reservoirs in developing quantum technology such as quantum computation and information.

ACKNOWLEDGMENTS

This work was supported by funds from the Wuhan University of Technology with Project Code No. 40120597, Project No. IBS-R024-D1, and the Korea Institute for Advanced Study (KIAS). H.C.P. acknowledges the hospitality at APCTP, where part of this work was done.

APPENDIX A: DERIVATION OF THE AMPLITUDE DISTRIBUTION COEFFICIENTS OF EIGENSTATES

From the definition of the Floquet operator $U(T_-, 0_-)$ and the chiral operator Γ , Eq. (8) can be written as follows:

$$\begin{aligned} & e^{-i(a^\dagger a + \sigma_z/2)2k\pi} e^{i2k\pi g(a\sigma_+ + a^\dagger\sigma_-)} |\phi_\alpha\rangle \\ & = e^{i\varepsilon_\alpha} e^{-i2k\pi\xi(a^\dagger + a)} |\phi_\alpha\rangle. \end{aligned} \quad (\text{A1})$$

Let us consider the eigenstates $|\psi_n\rangle$ and eigenenergy E_n of $H'_g = 2k\pi H_g = 2k\pi g(a\sigma_+ + a^\dagger\sigma_-)$ for calculating the amplitude distribution coefficients. The equation is written as

$$\begin{aligned} e^{i2k\pi g(a^\dagger\sigma_- + a\sigma_+)} |\phi_\alpha\rangle & = \sum_n e^{iE_n} \langle \psi_n | \phi_\alpha \rangle |\psi_n\rangle \\ & = \sum_n (C_n^+ \cos \beta_n + iC_{n+1}^- \sin \beta_n) |n, +\rangle \\ & \quad + \sum_n (C_{n+1}^- \cos \beta_n + iC_n^+ \sin \beta_n) |n+1, -\rangle, \end{aligned} \quad (\text{A2})$$

where $\beta_n = 2k\pi g\sqrt{n+1}$. Using this equation and the definition of D_n^\pm , from Eq. (A1), we can get the amplitude distribution coefficient of the chiral partner as follows:

$$D_n^+ = (-1)^k e^{-i\varepsilon_\alpha} [C_n^+ \cos \beta_n + iC_{n+1}^- \sin \beta_n], \quad (\text{A3})$$

$$D_{n+1}^- = (-1)^k e^{-i\varepsilon_\alpha} [C_{n+1}^- \cos \beta_n + iC_n^+ \sin \beta_n]. \quad (\text{A4})$$

Let us calculate the expectation values of the operators composed of the chiral operator and the coupling Hamiltonian as follows:

$$\begin{aligned} \mathcal{A} & = \langle \phi_\alpha | (a\sigma_+ + a^\dagger\sigma_-) e^{i\pi a^\dagger a} e^{-i2k\pi\xi(a^\dagger + a)} |\phi_\alpha\rangle \\ & = \sum_n (-1)^n \sqrt{n+1} [D_n^+ (C_{n+1}^-)^* - D_{n+1}^- (C_n^+)^*], \end{aligned} \quad (\text{A5})$$

$$\begin{aligned} \mathcal{B} & = \langle \phi_\alpha | e^{i2k\pi\xi(a^\dagger + a)} (a\sigma_+ + a^\dagger\sigma_-) e^{i\pi a^\dagger a} |\phi_\alpha\rangle \\ & = \sum_n (-1)^n \sqrt{n+1} [C_n^+ (D_{n+1}^-)^* - C_{n+1}^- (D_n^+)^*]. \end{aligned} \quad (\text{A6})$$

Since the expectation values are satisfied by $\mathcal{A} = \mathcal{B}$, we can get the following equation:

$$D_n^+ (C_{n+1}^-)^* - D_{n+1}^- (C_n^+)^* + C_{n+1}^- (D_n^+)^* - C_n^+ (D_{n+1}^-)^* = 0. \quad (\text{A7})$$

We can rewrite Eq. (A3) as

$$C_{n+1}^- = \frac{(-1)^k e^{i\varepsilon_\alpha} D_n^+ - C_n^+ \cos \beta_n}{i \sin \beta_n}, \quad (\text{A8})$$

and then substitute it into Eq. (A4) to get the coefficient

$$D_{n+1}^- = \frac{D_n^+ \cos \beta_n - (-1)^k e^{-i\varepsilon_\alpha} C_n^+}{i \sin \beta_n}. \quad (\text{A9})$$

Substituting Eqs. (A8) and (A9) into Eq. (A7), the relation between two coefficients is as follows:

$$\frac{(-1)^k (|D_n^+|^2 - |C_n^+|^2) (e^{i\varepsilon_\alpha} - e^{-i\varepsilon_\alpha})}{i \sin \beta_n} = 0, \quad (\text{A10})$$

which implies the simple relation

$$|D_n^+|^2 = |C_n^+|^2. \quad (\text{A11})$$

From Eqs. (A3) and (A4), the relation between $|D_n^+|^2$ and $|D_{n+1}^-|^2$ is written as

$$\begin{aligned} |D_n^+|^2 - |D_{n+1}^-|^2 &= (\cos^2 \beta_n - \sin^2 \beta_n) (|C_n^+|^2 - |C_{n+1}^-|^2) \\ &\quad + 2i \sin \beta_n \cos \beta_n [C_{n+1}^- (C_n^+)^* - C_n^+ (C_{n+1}^-)^*]. \end{aligned} \quad (\text{A12})$$

Equation (A12) gives

$$\begin{aligned} (|C_n^+|^2 - |C_{n+1}^-|^2) \sin \beta_n &= i \cos \beta_n [C_{n+1}^- (C_n^+)^* - C_n^+ (C_{n+1}^-)^*]. \end{aligned} \quad (\text{A13})$$

From Eq. (A13), we can rewrite

$$\begin{aligned} (-1)^k e^{-i\varepsilon_\alpha} (C_n^+)^* [\cos \beta_n C_{n+1}^- + i \sin \beta_n C_n^+] &= (-1)^k e^{-i\varepsilon_\alpha} (C_{n+1}^-)^* [\cos \beta_n C_n^+ + i \sin \beta_n C_{n+1}^-]. \end{aligned} \quad (\text{A14})$$

Using Eqs. (A3) and (A4), finally, we can get the relation between the amplitude distribution coefficients of the chiral partners as follows:

$$\frac{D_n^+}{D_{n+1}^-} = \left(\frac{C_n^+}{C_{n+1}^-} \right)^*. \quad (\text{A15})$$

APPENDIX B: DERIVATION OF STATE EVOLUTION

Considering a pair of eigenphases under chiral symmetry, Eq. (15) is rewritten as

$$\begin{aligned} |\Psi(M)\rangle &= \sum_{\alpha \in \mathbb{E}} (e^{-i\varepsilon_\alpha MT} \langle \phi_\alpha | \Psi(0) \rangle | \phi_\alpha \rangle \\ &\quad + e^{i\varepsilon_\alpha MT} \langle \phi_\alpha | \Gamma^\dagger | \Psi(0) \rangle \Gamma | \phi_\alpha \rangle), \end{aligned} \quad (\text{B1})$$

where \mathbb{E} is defined by a set of index α having positive energies including zero energy, $\mathbb{E} = \{\alpha | \varepsilon_\alpha \geq 0\}$, and we separate the eigenenergies as pairs under chiral symmetry. Let us take the n_0 th and even state $|\Psi(0)\rangle = e^{i\theta_0} |n_0, +\rangle$ as the initial state with an initial phase θ_0 , and use the relations of the amplitude distribution coefficients $D_n^\pm = |C_n^\pm| e^{i(\theta_\varepsilon - \theta_n^\pm)}$ and $C_n^\pm = |C_n^\pm| e^{i\theta_n^\pm}$. The element of the summation is written by

$$\begin{aligned} e^{-i\varepsilon_\alpha MT} \langle \phi_\alpha | \Psi(0) \rangle | \phi_\alpha \rangle &= \sum_{n, \eta = \pm} |C_{n_0}^+ C_n^\eta| e^{-i\varepsilon_\alpha MT + i\theta_0 - i\theta_{n_0}^+ + i\theta_n^\eta} |n, \eta\rangle, \end{aligned} \quad (\text{B2})$$

$$\begin{aligned} e^{i\varepsilon_\alpha MT} \langle \phi_\alpha | \Gamma^\dagger | \Psi(0) \rangle \Gamma | \phi_\alpha \rangle &= \sum_{n, \eta = \pm} |C_{n_0}^+ C_n^\eta| e^{i\varepsilon_\alpha MT + i\theta_0 + i\theta_{n_0}^+ - i\theta_n^\eta + i(n_0+n)\pi} |n, \eta\rangle, \end{aligned} \quad (\text{B3})$$

and then we can get the final wave function after MT ,

$$|\Psi(M)\rangle = \sum_{n, \pm} \mathcal{P}_n^\eta(M) |n, \eta\rangle, \quad (\text{B4})$$

where the amplitude function is as follows:

$$\begin{aligned} \mathcal{P}_n^\eta(M) &= \sum_{\alpha \in \mathbb{E}} [|C_{n_0}^+ C_n^\eta| e^{i\theta_0} e^{-i\mathcal{Q}_{n\alpha}^\eta(M)} \\ &\quad + |C_{n_0}^+ C_n^\eta| e^{i\theta_0 + i(n_0+n)\pi} e^{i\mathcal{Q}_{n\alpha}^\eta(M)}], \end{aligned} \quad (\text{B5})$$

where $\mathcal{Q}_{n\alpha}^\eta(M) = \varepsilon_\alpha MT + \theta_{n_0}^+ - \theta_n^\eta$ and \mathbb{E} is defined by a set of index α having positive energies including zero energy, $\mathbb{E} = \{\alpha | \varepsilon_\alpha \geq 0\}$. Finally, we get

$$\mathcal{P}_n^\eta(M) = e^{i\theta_0} \sum_{\alpha \in \mathbb{E}} [2 |C_{n_0}^+ C_n^\eta| \cos \mathcal{Q}_{n\alpha}^\eta(M)] \quad (\text{B6})$$

when $n_0 + n$ is an even number, and

$$\mathcal{P}_n^\eta(M) = e^{i(\theta_0 + \pi/2)} \sum_{\alpha \in \mathbb{E}} [-2 |C_{n_0}^+ C_n^\eta| \sin \mathcal{Q}_{n\alpha}^\eta(M)] \quad (\text{B7})$$

when $n_0 + n$ is an odd number.

-
- [1] E. T. Jaynes and F. W. Cummings, *Proc. IEEE* **51**, 89 (1963).
[2] B. W. Shore and P. L. Knight, *J. Mod. Opt.* **40**, 1195 (1993).
[3] A. Frisk Kockum, A. Miranowicz, S. De Liberato, S. Savasta, and F. Nori, *Nat. Rev. Phys.* **1**, 19 (2019).
[4] P. Forn-Díaz, L. Lamata, E. Rico, J. Kono, and E. Solano, *Rev. Mod. Phys.* **91**, 025005 (2019).
[5] J. C. Retamal and C. Saavedra, *Phys. Rev. A* **50**, 1867 (1994).
[6] G. Khitrova, H. Gibbs, M. Kira, S. W. Koch, and A. Scherer, *Nat. Phys.* **2**, 81 (2006).
[7] Y. Ota, R. Ohta, N. Kumagai, S. Iwamoto, and Y. Arakawa, *Phys. Rev. Lett.* **114**, 143603 (2015).
[8] K. Müller, A. Rundquist, K. A. Fischer, T. Sarmiento, K. G. Lagoudakis, Y. A. Kelaita, C. S. Muñoz, E. del Valle, F. P. Laussy, and J. Vučković, *Phys. Rev. Lett.* **114**, 233601 (2015).
[9] C. Hamsen, K. N. Tolazzi, T. Wilk, and G. Rempe, *Phys. Rev. Lett.* **118**, 133604 (2017).
[10] J. Tang, W. Geng, and X. Xu, *Sci. Rep.* **5**, 9252 (2015).
[11] P. Alsing and H. Carmichael, *Quantum Opt.: J. Eur. Opt. Soc. B* **3**, 13 (1991).
[12] F. P. Laussy, E. del Valle, M. Schropp, A. Laucht, and J. J. Finley, *J. Nanophoton.* **6**, 061803 (2012).
[13] C. S. Muñoz, F. P. Laussy, E. del Valle, C. Tejedor, and A. González-Tudela, *Optica* **5**, 14 (2018).
[14] M. D. Reed, L. DiCarlo, B. R. Johnson, L. Sun, D. I. Schuster, L. Frunzio, and R. J. Schoelkopf, *Phys. Rev. Lett.* **105**, 173601 (2010).
[15] S. Sun, H. Kim, G. S. Solomon, and E. Waks, *Phys. Rev. Appl.* **9**, 054013 (2018).
[16] M. Bukov, L. D'Alessio, and A. Polkovnikov, *Adv. Phys.* **64**, 139 (2015).
[17] T. Oka and S. Kitamura, *Annu. Rev. Condens. Matter Phys.* **10**, 387 (2019).
[18] D. W. Hone, R. Ketzmerick, and W. Kohn, *Phys. Rev. E* **79**, 051129 (2009).

- [19] E. J. Meier, J. Ang'ong'a, F. Alex An, and B. Gadway, *Phys. Rev. A* **100**, 013623 (2019).
- [20] K. Yang, L. Zhou, W. Ma, X. Kong, P. Wang, X. Qin, X. Rong, Y. Wang, F. Shi, J. Gong *et al.*, *Phys. Rev. B* **100**, 085308 (2019).
- [21] A. Dutt, M. Minkov, Q. Lin, L. Yuan, D. A. Miller, and S. Fan, *Nat. Commun.* **10**, 3122 (2019).
- [22] M. E. Tzur, O. Neufeld, E. Bordo, A. Fleischer, and O. Cohen, *Nat. Commun.* **13**, 1312 (2022).
- [23] J. Cayssol, B. Dóra, F. Simon, and R. Moessner, *Phys. Status Solidi RRL* **7**, 101 (2013).
- [24] N. H. Lindner, G. Refael, and V. Galitski, *Nat. Phys.* **7**, 490 (2011).
- [25] H. Wu and J.-H. An, *Phys. Rev. B* **102**, 041119(R) (2020).
- [26] W. Zhu, Y. D. Chong, and J. Gong, *Phys. Rev. B* **104**, L020302 (2021).
- [27] R. Moessner and S. L. Sondhi, *Nat. Phys.* **13**, 424 (2017).
- [28] W. Kohn, *J. Stat. Phys.* **103**, 417 (2001).
- [29] G. B. Cuetara, A. Engel, and M. Esposito, *New J. Phys.* **17**, 055002 (2015).
- [30] G. Casati, B. V. Chirikov, F. M. Izraelev, and J. Ford, *Stochastic Behavior in Classical and Quantum Hamiltonian Systems: Volta Memorial Conference, Como, 1977* (Springer-Verlag, Berlin, 1979).
- [31] P. Qin, A. Andreanov, H. C. Park, and S. Flach, *Sci. Rep.* **7**, 41139 (2017).
- [32] M. J. Moeckel, D. R. Southworth, E. M. Weig, and F. Marquardt, *New J. Phys.* **16**, 043009 (2014).
- [33] P. Qin and H. C. Park, *Phys. Rev. B* **104**, 064303 (2021).
- [34] P. Hosur, S. Ryu, and A. Vishwanath, *Phys. Rev. B* **81**, 045120 (2010).
- [35] J. K. Asbóth and H. Obuse, *Phys. Rev. B* **88**, 121406(R) (2013).
- [36] C.-K. Chiu, J. C. Y. Teo, A. P. Schnyder, and S. Ryu, *Rev. Mod. Phys.* **88**, 035005 (2016).
- [37] T. Kitagawa, E. Berg, M. Rudner, and E. Demler, *Phys. Rev. B* **82**, 235114 (2010).
- [38] G. Zaslavskii, M. Y. Zakharov, R. Sagdeev, D. Usikov, and A. Chernikov, *Sov. Phys. JETP* **64**, 294 (1986).
- [39] R. Lima and D. Shepelyansky, *Phys. Rev. Lett.* **67**, 1377 (1991).
- [40] T. Geisel, R. Ketzmerick, and G. Petschel, *Phys. Rev. Lett.* **67**, 3635 (1991).
- [41] D. Y. Ho and J. Gong, *Phys. Rev. B* **90**, 195419 (2014).
- [42] P. H. Jones, M. M. Stocklin, G. Hur, and T. S. Monteiro, *Phys. Rev. Lett.* **93**, 223002 (2004).
- [43] J. Wang and J. Gong, *Phys. Rev. A* **77**, 031405(R) (2008).
- [44] L. Zhou and J. Gong, *Phys. Rev. A* **97**, 063603 (2018).
- [45] Y. Aharonov, L. Davidovich, and N. Zagury, *Phys. Rev. A* **48**, 1687 (1993).
- [46] M. S. Rudner and L. S. Levitov, *Phys. Rev. Lett.* **102**, 065703 (2009).
- [47] T. Oka, N. Konno, R. Arita, and H. Aoki, *Phys. Rev. Lett.* **94**, 100602 (2005).
- [48] M. Karski, L. Förster, J.-M. Choi, A. Steffen, W. Alt, D. Meschede, and A. Widera, *Science* **325**, 174 (2009).
- [49] A. Blais, R.-S. Huang, A. Wallraff, S. M. Girvin, and R. J. Schoelkopf, *Phys. Rev. A* **69**, 062320 (2004).
- [50] B. Gadway, J. Reeves, L. Krinner, and D. Schneble, *Phys. Rev. Lett.* **110**, 190401 (2013).
- [51] G. Floquet, in *Annales Scientifiques de l'École Normale Supérieure* (1883), Vol. 12, pp. 47–88.
- [52] J. H. Shirley, *Phys. Rev.* **138**, B979 (1965).
- [53] Y. B. Zel'Dovich, *Sov. Phys. JETP* **24**, 1006 (1967).
- [54] V. I. Ritus, *Sov. Phys. JETP* **24**, 1041 (1967).